



ALMA MATER STUDIORUM  
UNIVERSITÀ DI BOLOGNA

ARCHIVIO ISTITUZIONALE  
DELLA RICERCA

## Alma Mater Studiorum Università di Bologna Archivio istituzionale della ricerca

Accuracy Evaluation of an Equivalent Synchronization Method for Assessing the Time Reference in Power Networks

This is the final peer-reviewed author's accepted manuscript (postprint) of the following publication:

*Published Version:*

Mingotti, A., Peretto, L., Tinarelli, R. (2018). Accuracy Evaluation of an Equivalent Synchronization Method for Assessing the Time Reference in Power Networks. IEEE TRANSACTIONS ON INSTRUMENTATION AND MEASUREMENT, 67(3), 600-606 [10.1109/TIM.2017.2779328].

*Availability:*

This version is available at: <https://hdl.handle.net/11585/621782> since: 2020-05-20

*Published:*

DOI: <http://doi.org/10.1109/TIM.2017.2779328>

*Terms of use:*

Some rights reserved. The terms and conditions for the reuse of this version of the manuscript are specified in the publishing policy. For all terms of use and more information see the publisher's website.

This item was downloaded from IRIS Università di Bologna (<https://cris.unibo.it/>).  
When citing, please refer to the published version.

(Article begins on next page)

# Accuracy Evaluation of an Equivalent Synchronization Method for Assessing the Time Reference in Power Networks

Alessandro Mingotti<sup>1</sup>, *Student Member, IEEE*, Lorenzo Peretto, *Senior Member, IEEE*,  
and Roberto Tinarelli, *Senior Member, IEEE*

**Abstract**—This paper deals with the evaluation of the accuracy performance of an approach for assessing the phase displacement between voltages at power network nodes. This task is accomplished by processing asynchronous measurements taken at each node. This turns into an equivalent synchronization, which is, therefore, obtained without exploiting any synchronization signals, such as the ones provided by means of wireless (i.e., global positioning system) or wired technologies. As a matter of fact, distribution system operators will gain the possibility of deploying, at more affordable costs, wide area measurement system (WAMS) over their power networks for enhancing their stability and reliability. Phasor measurement units (PMUs) are the most common examples of such WAMS, but, besides their high cost, there are circumstances where providing a time reference signal to remote PMUs often becomes a difficult task. This paper aims at recalling the basic theoretical principles of the method and at proving its applicability in power network through a deep analysis of its metrological performance.

**Index Terms**—Accuracy evaluation, asynchronous measurement, network impedance, phase angle measurement, phase difference, phasor measurement units (PMUs), time synchronization, uncertainty.

## I. INTRODUCTION

WITH the huge and fast development of smart grids and distributed generation, the need to perform measurements in many different nodes of the power networks has become a paramount importance for distribution system operators to allow an effective control of the network operation. Furthermore, the possibility to also synchronize measurements performed at different nodes of the power networks has allowed even to improve the control performance: better control of the operation frequency, fault detection and location, higher network stability, islanding detection and operation, improving the power flow in the network, etc.

As well known, the devices that allow to perform synchronized measurements in power networks are referred to as phasor measurement units (PMUs) [1]. They allow not only to perform the measurement of the rms value of the voltages and currents but also of their phases with respect to

a global time reference. This way, according to the definition of phasor given by Steinmetz [2] in 1893, the phasor of a voltage or a current is given by its rms value and by its phase difference with respect to a defined time reference. The comparison between the phases of all voltages in a power network allows to evaluate the state estimation of the network, which, in turn, represents the gate for getting the observability of the whole network. So, the added value of a PMU with respect to a typical power meter is given by the possibility to evaluate the phase difference of all voltages in a network, which is accomplished by means of a global time reference.

The use of PMUs in transmission lines started around 1988 and its usefulness for a better network control and monitoring is today well recognized. In transmission lines, the errors allowed in the evaluation of phase displacement between voltages are not a critical parameter due to the very long distances and then to the large difference of the voltage phases (in the order of tens of mrad/km). So, traditional voltage transformers (VTs) with 0.2 accuracy class, used for billing purposes, result well suitable for such an application.

However, in distribution networks this is not likely to happen. The use of PMUs in such kind of networks has been widely investigated in the scientific literature also from the measurement point of view (see [3]–[5]). But distribution lines are far shorter than transmission ones and the difference between the node voltage phases results often very small, in the order of very few milliradian per kilometer. Hence, VTs with typical 0.5 accuracy class already installed for billing purposes and measurement in general are no longer suitable for PMU usage. In conclusion, besides the need to have an accurate time reference (with standard deviation in the order of 1  $\mu$ s or lower) also very accurate VTs are required for assuring a properly accurate evaluation of the voltage phasors. Of course, noticeable contribution to the study of how the uncertainty in the measurement hardware affects the results provided by the PMU-based system has been given by the measurement community, as proved in [6]–[8].

Nowadays the global time reference can be provided to all PMUs deployed in the network by means of wireless or wired communication protocols. The pulse-per-second information included in the global positioning system (GPS) signals represents the worldwide most used time reference information. It can be easily and freely read by means of antennas and receivers for triggering all PMUs to a unique reference.

Manuscript received July 12; revised September 9, 2017; accepted September 10, 2017. The Associate Editor coordinating the review process was Dr. Jesús Ureña. (*Corresponding author: Alessandro Mingotti.*)

The authors are with the Department of Electrical, Electronic and Information Engineering G. Marconi, Alma Mater Studiorum–University of Bologna, 40126 Bologna, Italy.

Color versions of one or more of the figures in this paper are available online at <http://ieeexplore.ieee.org>.

Digital Object Identifier 10.1109/TIM.2017.2779328

85 Among many advantages in using such a technique, it shows,  
 86 on the contrary, some criticalities: the most important one is  
 87 represented by the need to install the antenna such that to be  
 88 able to receive satellite signals. But this is not always occurring  
 89 in many circumstances, like, for instance, in urban areas,  
 90 where many obstacles can make it difficult: trees, buildings,  
 91 skyscrapers, underground secondary substations, roads, and  
 92 others. In such situations, there is a need of a periodical  
 93 calibration of the PMUs internal clock, by means, for example,  
 94 of a traveling standard [9].

95 In the last decade also wired time reference infrastructures  
 96 have been developed. Today their performance (in terms of  
 97 delays and accuracy of the time reference) is getting more and  
 98 more close to the GPS one. In particular, the IEEE 1588 [10]  
 99 and IEC 61850-5 [11] Standards are by far the most used  
 100 recommend practices for the transmission of reference times  
 101 over wired communication infrastructures [12]. However, also  
 102 such a technology shows some limitations. In particular, they  
 103 are cost effective in case of a lack of a suitable communication  
 104 network. Moreover, in rural areas the deployment of a wiring  
 105 infrastructure can result almost impossible.

106 At the light of all the aforementioned issues, a novel  
 107 analytical method for assessing the phase difference between  
 108 voltages at different nodes of a distribution power network  
 109 has been proposed in [13], of which this paper is a technical  
 110 extension. The main feature of such a method is that no global  
 111 time reference is required for triggering the measurement units  
 112 deployed in the field. Measurements at different nodes are  
 113 performed asynchronously. It only requires that voltages and  
 114 currents in each node of the networks are simultaneously  
 115 acquired. This task is generally accomplished by commercial  
 116 power meters.

117 The implementation of such a method is beneficial in  
 118 all situations where synchronization signals are not avail-  
 119 able or (and) a less expensive measurement architecture is  
 120 required.

121 In the scientific literature, only one application of unsyn-  
 122 chronized measurement of phasors in power networks can be  
 123 found, i.e., in [14]. In [14], Janssen *et al.* iteratively determine  
 124 the state of the network formulated by means of the so-  
 125 called augmented matrix approach. On the contrary, several  
 126 papers (see [15]–[22]) exploit unsynchronized measurements  
 127 to tackle fault location issues.

128 In [13], the performance of the proposed method has been  
 129 evaluated by comparing the phase displacements provided by  
 130 the method with actual ones in different simulated power  
 131 network conditions. The obtained results look satisfactory,  
 132 but in order to asses if the proposed approach can be an  
 133 effective alternative to conventional synchronization methods  
 134 (like GPS-based solutions), further investigations are required.  
 135 To this purpose, in this paper a typical configuration of the  
 136 measurement system, which allows getting the information  
 137 required for applying the proposed equivalent synchronization  
 138 method, is considered. Different scenarios, each of them char-  
 139 acterized by different accuracies of the measurement devices,  
 140 are analyzed to evaluate the overall accuracy of the proposed  
 141 approach under actual conditions.

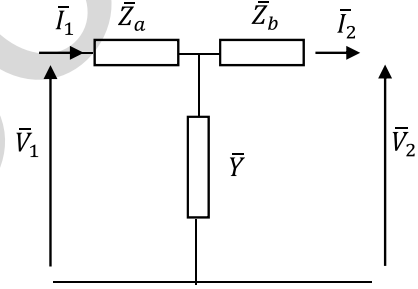


Fig. 1. T-circuit representation of single-wire line.

This paper is structured as follows. In Section II, the method  
 presented in [13] is recalled, whereas in Section III the  
 configuration of the measurement system is described.

A brief summary of uncertainty evaluation methods  
 designed for this purpose is presented in Section IV. Numerical  
 results of different scenarios are shown and discussed in  
 Section V. Finally, conclusions are drawn in Section VI.

## II. PROPOSED APPROACH

### A. Theoretical Background: Electric Line Modeling

Let us briefly recall how an electric line is modeled. As is  
 well known, it can be represented by the equivalent circuit  
 in Fig. 1, where the following notations are used.

- 1)  $\bar{V}_1$  and  $\bar{V}_2$  are the voltage phasors at the beginning  
 (node 1) and the end (node 2), respectively.
- 2)  $\bar{I}_1$  and  $\bar{I}_2$  are the current phasors getting out the node 1  
 and getting in the node 2, respectively.
- 3)  $\bar{Z}_a$ ,  $\bar{Z}_b$ , and  $\bar{Y}$  are the equivalent parameters of the above  
 obtained T-circuit, as briefly described in the following,  
 from the two-port model matrix.

Such a matrix relates  $\bar{V}_1$  and  $\bar{I}_1$  with  $\bar{V}_2$  and  $\bar{I}_2$

$$\begin{bmatrix} \bar{V}_2 \\ \bar{I}_2 \end{bmatrix} = \begin{bmatrix} \bar{A} & -\bar{B} \\ -\bar{C} & \bar{A} \end{bmatrix} \begin{bmatrix} \bar{V}_1 \\ \bar{I}_1 \end{bmatrix}. \quad (1)$$

In (1)

$$\bar{A} = \cosh(\bar{\gamma}l) \quad (2)$$

$$\bar{B} = \bar{Z}_c \sinh(\bar{\gamma}l) \quad (3)$$

$$\bar{C} = \bar{Y}_c \sinh(\bar{\gamma}l) \quad (4)$$

with  $l$  the length of the line and  $\bar{\gamma}$  the propagation constant  
 which depends on the per unit length parameters  $r$ ,  $l$ ,  $c$ , and  $g$   
 (usually  $g$  is neglected in medium voltage cables).

Once  $\bar{A}$ ,  $\bar{B}$ , and  $\bar{C}$  are known, the parameters of the  
 equivalent circuit can be computed as follows:

$$\bar{Z}_a = \bar{Z}_b = \frac{\bar{A} - 1}{\bar{C}} \quad (5)$$

$$\bar{Y} = \bar{C}. \quad (6)$$

### B. Procedure

As mentioned in Section I, the main goal of this paper is  
 the estimation of the phase displacement between voltage  $\bar{V}_1$   
 at the beginning of the line, taken as reference, and voltage  $\bar{V}_2$   
 at the end of the line without using synchronized measurements



Fig. 2. Single-wire line topology.

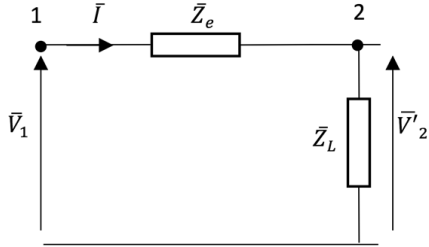


Fig. 3. Representation of a single-wire line and its load used in the proposed approach.

(Fig. 2). It must be underlined that as it will become more clear in the following, the proposed procedure can be applied (hence it is suitable) for state estimation of power networks under steady-state conditions, like for instance in all applications required by SCADA systems.

Besides the state estimation, the presented approach can be also successfully used for diagnostic purposes. For instance, it allows the evaluation of resistive and reactive losses of power lines. Nowadays, this knowledge represents one of the most important requirements that utilities are looking for in network monitoring systems for smart grids.

According to the proposed approach, measurements in every node are performed and transmitted asynchronously every few seconds, in compliance with SCADA specifications. On the contrary, the presented method is not suitable for network monitoring under transient conditions (hence for protection purposes).

The phase displacement between voltages in the network is usually due to the combined effect of both the line (according to its model shown in Fig. 1) and the equivalent impedance  $\bar{Z}_L$  of the load connected at the end of line. The lack of synchronization does not allow to write a sufficient number of independent equations to determine all the three unknown parameters ( $Z_L$ ,  $Z_a = Z_b$ , and  $Y$ ) of such a circuit. Therefore, the proposed method relies on the use of a different model, shown in Fig. 3, where  $\bar{Z}_e$  is an equivalent impedance of the line computed in a such a way that line losses as well as the active powers at nodes 1 and 2 are the same as the actual ones. As a matter of fact, active power is an integral quantity computed over one (or more) cycles and its value at such nodes is independent from the synchronization of its measurements, pending the power system is in steady-state conditions for just one cycle in each node.

In the following, the procedure for estimating the searched phase difference is recalled. To this purpose, let us denote by  $\Delta\varphi_a$  the actual value of such a phase difference and by  $\Delta\varphi_e$  the corresponding estimate provided by the equivalent synchronization approach.

First of all, the couple of phasors  $\bar{V}_1$  and  $\bar{I}_1$ ,  $\bar{V}_2$  and  $\bar{I}_2$  must be measured. In each measurement node, voltage and current

are simultaneously acquired, so that the relationship between the phasors of each couple is correct. Of course, due to the lack of synchronization, the phase displacement between  $\bar{V}_1$  and  $\bar{V}_2$  is  $\Delta\varphi_a + \delta$ , where  $\delta$  is a random angle depending on the random time difference between the acquisition of the two couples of phasors.

With reference to the circuit in Fig. 3, the following system of equations can be written:

$$\begin{cases} P'_2 = \text{Re} \left( \frac{|\bar{V}'_2|^2}{\bar{Z}_L^*} \right) \\ \bar{V}'_2 = \bar{V}_1 \frac{\bar{Z}_L}{\bar{Z}_L + \bar{Z}_e} = \bar{V}_1 \frac{\bar{Z}_L}{\bar{Z}_L + R_e + jX_e} \end{cases} \quad (7)$$

where  $P'_2$  is the active power at node 2 of such a circuit and  $R_e$  and  $X_e$  are the resistance and reactance of the equivalent impedance  $\bar{Z}_e$ . Given that, as stated above,  $P'_2 = P_2$  and measurements of  $\bar{V}_2$  and  $\bar{I}_2$  allow the determination of the actual value of  $\bar{Z}_L$

$$\bar{Z}_L = \frac{\bar{V}_2}{\bar{I}_2}. \quad (8)$$

The only unknowns of (7) are  $\bar{V}'_2$  and  $\bar{Z}_e$ . As for  $\bar{Z}_e$ , the resistive part  $R_e$  can be determined under the assumption of the same line losses in both circuits of Figs. 1 and 3

$$R_e = 2 \frac{P_1 - P_2}{I_1^2 + I_2^2} \quad (9)$$

where  $P_1$  and  $P_2$  are the active powers measured at nodes 1 and 2, respectively, and  $I_1$  and  $I_2$  are the rms values of the above-defined current phasors.

By substituting the second equation of (7) into the first one, the reactive part  $X_e$  of  $\bar{Z}_e$  can be obtained by solving the following second-order equation [5]:

$$X_e^2 + 2X_e X_L + d = 0 \quad (10)$$

where  $X_L$  is the reactive part of  $\bar{Z}_L$  and

$$d = |\bar{Z}_L|^2 - \frac{|\bar{V}_1|^2 |\bar{Z}_L|^2}{P_2} \text{Re} \left\{ \frac{1}{\bar{Z}_L^*} \right\} + R_e \bar{Z}_L^* + R_e \bar{Z}_L + R_e^2. \quad (11)$$

One of the solutions of (10) is always negative if, as it is usual, the power factor of  $\bar{Z}_L$  is lagging.

Finally,  $\bar{V}'_2$  can be determined along with its phase displacement  $\Delta\varphi_e$ , with respect to  $\bar{V}_1$  by means of the second equation of (7).

### III. MEASUREMENT SYSTEM CONFIGURATION

The implementation of the proposed equivalent synchronization approach requires the use of a wide area measurement system which, conversely to those based on PMUs, does not require any kind of synchronization among different remote units. In the scientific literature, several applications of distributed measurement systems can be found for two main purposes: 1) for monitoring periodic disturbances and try to determine their sources [23], [24] and 2) for locating the faults caused by internal (i.e., line fault [25], [26]) and

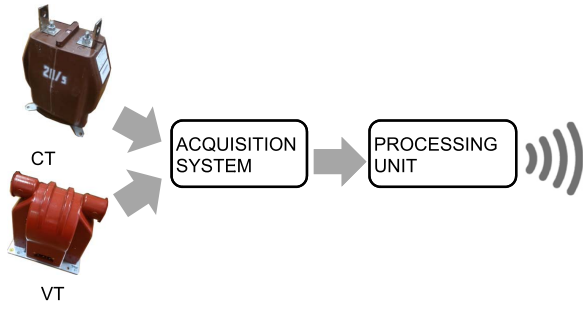


Fig. 4. Schematic representation of the measurement system configuration.

external (i.e., lighting [27]) sources. Both situations require synchronization between the different remote units. The lack of such a requirement has to be investigated [28] as well as the overall metrological performance of the system [29]. The proposed system consists of a main unit and many remote units as the number of the monitored nodes (two in the considered examples). Each remote unit consists of three VTs, three current transformers (CTs), an acquisition system, a processing unit, and a transmission device, as shown in Fig. 4. VT and CT may be inductive instrument transformers (ITs) [30] or low-power ITs [31] and can be considered as the main sources of uncertainty. As for the acquisition system, it must feature simultaneous sampling of its inputs in order to avoid any additional phase errors. Commercial devices can easily ensure time delay on the order of very few microseconds (about 0.3 mrad at 50 Hz). Moreover, the use of a phase-locked loop results in negligible effects of leakage errors. This solution is already implemented in many instrument used in power system, such as, for example, several commercial digital energy meters. The processing unit computes voltage and current phasors from the sequence representing voltage and current waveforms. Finally, the transmission device sends the above phasors to the main unit by exploiting some kind of communication technology and protocol. The way the information is sent is outside the purpose of this paper.

The main unit collects the voltage and current phasors coming from all the nodes and determines  $\Delta\varphi_e$  by applying the procedure described in Section II-B.

#### IV. UNCERTAINTY EVALUATION METHODS

According to the “Guide to the expression of Uncertainty in Measurements” and its Supplement 1 [32], [33], the result  $Y$  of a measurement is a random variable.  $Y$  is a function  $f$  of the input quantities  $X_i$ . As it is well known, random variables can be used to represent both random and systematic effects. The first one is caused by unpredictable changes in the experiment, while the second originates from the measuring instruments.

According to [32] and [33], the pdf associated with  $Y$  is determined by a combination of the pdfs associated with each  $X_i$ . However, if the operation between the pdfs is different from the sum of two pdfs, which turns into the convolution of them, there is not any mathematical approach to deal with such pdfs. In order to solve this issue, [32] and [33] propose two different solutions.

TABLE I  
ACTUAL AND ESTIMATED VOLTAGE PHASE DIFFERENCE  
FOR A 500-KVA LOAD, 10-KM LENGTH CABLE

S (mm <sup>2</sup> )	$\Delta\varphi_a$ (mrad)	$\Delta\varphi_e$ (mrad)	$\Delta\varphi_e - \Delta\varphi_a$ (mrad)
50	3.47	5.31	1.84
95	0.69	1.485	1.415

TABLE II  
PER UNIT LENGTH PARAMETERS FOR THE TWO TYPES OF CABLES

S (mm <sup>2</sup> )	r (mΩ/m)	l (μH/m)	c (nF/m)
50	0.587	0.4138	0.21
95	0.193	0.3694	0.26

- 1) GUM [32] presents an analytical approach, which provides exact results only in a restricted number of situations. It consists in the propagation of the mean and standard deviation of the pdfs along the measurement function, by means of a first-order Taylor series.
- 2) Supplement 1 [33] deals with a numerical simulation, the Monte Carlo method (MCM). Conversely to the previous approach, the MCM can be applied to a huge number of situations and, if well implemented, it features very accurate estimations.

Due to this fact, for the approach presented in this paper,  $f$  cannot be easily expressed, the MCM is the most suitable approach for tackling the uncertainty evaluation and propagation.

#### V. NUMERICAL EXAMPLES

In [13], the performance of the proposed approach has been tested in several conditions characterized by different cable cross sections, cable lengths, and apparent powers of the load. The results have been generally satisfactory (with an error ranging from 0.3 to 1.84 mrad) and it has been highlighted that the difference  $\Delta\varphi_e - \Delta\varphi_a$  (which represents the error of the method):

- 1) increases as the length of the line increases;
- 2) decreases as the cable cross section increases;
- 3) slightly decreases as the apparent power of the load increases.

At the light of the above outcomes, the uncertainty evaluation is focused on the worst of the previous studied cases: the longest line (10 km), the lowest apparent power (500 kVA), and the smallest cross sections (50 and 95 mm<sup>2</sup>). The errors  $\Delta\varphi_e - \Delta\varphi_a$  obtained in [13] for the above configurations are recalled in Table I, whereas Table II shows the per unit length parameters of the two cable cross sections considered.

For the sake of simplicity but without loss of generality, a single-phase configuration is considered, so that the contribution to uncertainty of only a VT, CT, and of the acquisition system must be taken into account. As for ITs, their accuracy performances are expressed by their accuracy classes as defined in [34] and [35] for inductive current and VTs, respectively. Accuracy classes provide limits for ratio and phase errors. Table III shows, for each accuracy class,



TABLE III  
RATIO ERRORS AND PHASE ERRORS FOR CT AND VT

Accuracy Class	$\epsilon_{CT}$ (%)	$\epsilon_{VT}$ (%)	$\Delta\phi_{CT}$ (crad)	$\Delta\phi_{VT}$ (crad)
0.1	0.1	0.1	0.15	0.15
0.2	0.2	0.2	0.3	0.3
0.5	0.5	0.5	0.9	0.6

ratio error  $\epsilon_{VT}$ , phase error  $\Delta\phi_{VT}$  and ratio error  $\epsilon_{CT}$ , phase error  $\Delta\phi_{CT}$  for VT and CT, as reported in [34] and [35], respectively.

As far as the acquisition system is concerned, the delay due to the noncomplete simultaneous sampling is neglected given that, as mentioned above, it turns into a phase error quite lower than the ones due to the ITs. Contributions due offset errors are not considered given that, as it is well known, they do not affect the phasors  $\bar{V}_1$ ,  $\bar{V}_2$ ,  $\bar{I}_1$ , and  $\bar{I}_2$ , when computed by means of the discrete Fourier transform algorithm. Therefore, only an overall contribution due to nonlinearity, gain, noise, and quantization, which is chosen equal to  $\pm 0.05\%$ , is taken into account. Such a value is consistent with that required by the largest Italian utility for its fault detection and power meters (see [36]).

For both the cable cross sections considered, different scenarios are analyzed. Each scenario is characterized by a CT and a VT featuring the same accuracy class, as usual in actual situations. Hence, according to Table III, three scenarios arise, in which, first the limits of the 95% confidence interval of  $\Delta\phi_e - \Delta\phi_a$  is evaluated (case #1). Then, it is studied how the different uncertainty sources located in the ITs contribute to the above interval. To this purpose, the following cases are analyzed:

- 1) only the sources located in the VT are considered (case #2);
- 2) only the sources located in the CT are considered (case #3);
- 3) only phase error of the VT is considered (case #4);
- 4) only ratio error of the VT is considered (case #5);
- 5) only phase error of the CT is considered (case #6);
- 6) only ratio error of the CT is considered (case #7).

All the uncertainty evaluation is performed by running a Monte Carlo simulation with 100000 iterations. According to [33], in the lack of any further information, each random variable, representing a contribution to uncertainty, is assumed to be uniformly distributed with zero mean and limits equal to the rated values of the considered contributions. A unimodal random variable (like all random variables considered in this paper), with uniform distribution, features the highest dispersion hence, according to the maximum entropy principle, in case of lack of information regarding the pdf of a random variable, uniform distribution has to be assumed.

Table IV lists, for the 50-mm<sup>2</sup> cable, the limits of the 95% confidence interval for the aforementioned seven cases of each of the three scenarios. The same quantities are shown in Table V for the 95-mm<sup>2</sup> cable. The first comment is that, as it is expected, uncertainty on  $\Delta\phi_e - \Delta\phi_a$ , which is reported in row named #1 of Tables IV and V in terms of limits of the

TABLE IV  
LIMITS (mrad) OF THE 95% CONFIDENCE INTERVAL OF PHASE DISPLACEMENT  $\Delta\phi_e$ , IN THE CASE OF A 50-mm<sup>2</sup> CABLE, FOR DIFFERENT ACCURACY CLASSES

CASE	0.1	0.2	0.5
#1	-2.10; 5.80	-6.10; 9.80	-18.1; 21.9
#2	-0.36; 4.00	-2.60; 6.30	-7.00; 10.7
#3	-1.40; 5.10	-4.60; 8.30	-15.9; 19.6
#4	-0.34; 4.00	-2.50; 6.20	-6.90; 10.6
#5	1.60; 2.00	1.40; 2.30	0.82; 2.90
#6	-0.35; 4.00	-2.50; 6.20	-11.3; 15.0
#7	-0.41; 4.10	-2.7; 6.40	-9.40; 13.2

TABLE V  
LIMITS (mrad) OF THE 95% CONFIDENCE INTERVAL OF PHASE DISPLACEMENT  $\Delta\phi_e$ , IN THE CASE OF A 95-mm<sup>2</sup> CABLE, FOR DIFFERENT ACCURACY CLASSES

CASE	0.1	0.2	0.5
#1	-2.50; 5.40	-6.50; 9.30	-18.6; 21.4
#2	-0.74; 3.60	-2.90; 5.70	-7.30; 10.1
#3	-1.80; 4.70	-5.00; 7.90	-16.4; 19.2
#4	-0.73; 3.60	-2.90; 5.70	-7.20; 10.0
#5	1.20; 1.70	0.92; 1.90	0.18; 2.70
#6	-0.74; 3.60	-2.90; 5.70	-11.5; 14.3
#7	-0.89; 3.70	-3.20; 6.00	-10.1; 13.0

95% confidence interval, increases as the accuracy class moves from 0.1 to 0.5. Moreover, it seems to be not significantly dependent on the cross section. By comparing case #2 with case #3 it can be stated that the contribution to uncertainty of the CT is greater than that of VT: in fact, the amplitude of the confidence interval of  $\Delta\phi_e - \Delta\phi_a$  obtained by considering only ratio and phase errors of the CT is about 1.5 times larger than the one obtained when only the VT accuracy is taken into account. This is justified by the fact that the quantity measured by the CTs (current phasor), on the contrary to the quantity (voltage phasor) measured by the VTs, appears also in terms of rms value in the evaluation of  $R_e$  [see (9)]. Such an explanation is confirmed by noticing that (see cases #3 and #4) the contribution to uncertainty due to the ratio error of the CTs is greater than that of VTs. As for cases #6 and #7, which represent the contribution of the phase errors, no significant dissimilarities between CT and VT can be appreciated, except for the 0.5 accuracy class where, according to Table III, the limits of the phase error are different for CT and VT.

As a final comment about the effect of the ITs accuracy, the analysis of the confidence interval widths, shown in Tables IV and V, highlights that only ITs featuring 0.1 or 0.2 accuracy class can be employed in actual application of the proposed approach.

On the basis of the procedure described in Section II-B, the evaluation of  $\Delta\phi_e$  relies on several quantities that are estimated by processing voltage and current phasors measured at the two nodes. Among such parameters, it can be observed that  $R_e$  and  $X_e$  can be derived in a different way if some

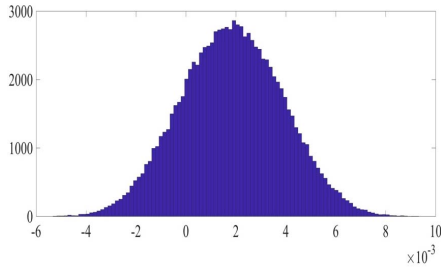


Fig. 5. Pdf of  $\Delta\varphi_e - \Delta\varphi_a$  for case #1 with 0.1 accuracy class.

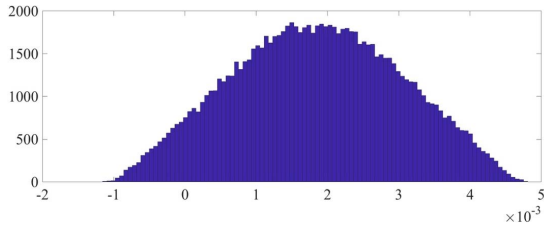


Fig. 6. Pdf of  $\Delta\varphi_e - \Delta\varphi_a$  for case #2 with 0.1 accuracy class.

information about the cable characteristics are provided. For example, with reference to the case #1 of Table IV, the limits of the confidence interval of  $\Delta\varphi_e - \Delta\varphi_a$  become  $-0.34; 4$  if  $R_e$  is known with an accuracy of  $\pm 10\%$  and  $X_e$  is evaluated according to (10). Such limits are  $0.17; 3.5$  when  $X_e$  is assumed to be known within  $\pm 10\%$  and  $R_e$  computed as in (9). Finally, the confidence interval of  $\Delta\varphi_e - \Delta\varphi_a$  is only  $1.5; 2.3$  when both the above parameters are provided with a  $\pm 10\%$  accuracy.

Figs. 5 and 6 show the estimated probability density function (pdf) for cases #1 and #2, respectively, when the accuracy class is 0.1 for both the ITs and the cross section is  $50 \text{ mm}^2$ . It can be observed that the pdf in Fig. 5 is approximately normal, whereas the one in Fig. 6 is almost trapezoidal. Of course, this is in accordance with the central limit theorem, given that the pdf in Fig. 5 refers to a random variable, which is obtained by the combination of more contributions to uncertainty.

All the uncertainty intervals associated with the phase displacement, have been obtained by assuming the worst case for the probability distribution of the random variables related to the uncertainty terms. This, according to the GUM, has to be considered the most likelihood confidence interval.

## VI. FINAL REMARKS AND FUTURE WORK

In this paper, an approach for assessing the phase displacement between voltages at power network nodes by processing asynchronous measurements in each node has been recalled. Starting from the description of the distributed measurement system that can be used to implement the recalled method, uncertainty affecting the errors in the estimate of the voltage phase displacements has been investigated in different operating conditions. Moreover, the contribution to the above uncertainty, due to each uncertainty source arising in the

measurement chain, has been evaluated. In the light of the obtained results concerning uncertainty evaluation, it can be concluded that the proposed approach can be assumed suitable for being extended to more complex power networks. In such cases, the proposed approach would be iteratively applied.

In the end, it has been highlighted that if the parameters characterizing the power cable are assumed to be known with an accuracy of  $\pm 10\%$ , the amplitude of the confidence interval on the error in the phase displacement measurement is significantly reduced. This is not an unrealistic assumption that will be subjected to future investigations.

## REFERENCES

- [1] A. Monti, C. Muscas, and F. Ponci, *Phasor Measurement Units and wide area Monitoring Systems: From the Sensors to the System*. New York, NY, USA: Elsevier, 2016.
- [2] C. P. Steinmetz, "Complex quantities and their use in electrical engineering," in *Proc. Int. Elect. Congr. (AIEE)*, 1893, pp. 33–74.
- [3] P. Castello, J. Liu, C. Muscas, P. A. Pegoraro, F. Ponci, and A. Monti, "A fast and accurate PMU algorithm for P+M class measurement of synchrophasor and frequency," *IEEE Trans. Instrum. Meas.*, vol. 63, no. 12, pp. 2837–2845, Dec. 2014.
- [4] A. Carta, N. Locci, and C. Muscas, "A PMU for the measurement of synchronized harmonic phasors in three-phase distribution networks," *IEEE Trans. Instrum. Meas.*, vol. 58, no. 10, pp. 3723–3730, Oct. 2009.
- [5] P. A. Pegoraro, A. Meloni, L. Atzori, S. Sulis, and P. Castello, "PMU-based distribution system state estimation with adaptive accuracy exploiting local decision metrics and IoT paradigm," *IEEE Trans. Instrum. Meas.*, vol. 66, no. 4, pp. 704–714, Apr. 2017.
- [6] J. Tang, J. Liu, F. Ponci, C. Muscas, and S. Sulis, "Effects of PMU's uncertainty on voltage stability assessment in power systems," in *Proc. IEEE Int. Instrum. Meas. Technol. Conf.*, May 2011, pp. 1–5.
- [7] C. Muscas, M. Pau, P. A. Pegoraro, and S. Sulis, "Uncertainty of voltage profile in PMU-based distribution system state estimation," *IEEE Trans. Instrum. Meas.*, vol. 65, no. 5, pp. 988–998, May 2016.
- [8] M. Asprou, E. Kyriakides, and M. Albu, "The effect of PMU measurement chain quality on line parameter calculation," in *Proc. IEEE Int. Instrum. Meas. Technol. Conf.*, May 2017, pp. 1–6.
- [9] A. Carullo, M. Parvis, and A. Vallan, "A GPS-synchronized traveling standard for the calibration of distributed measuring systems," in *Proc. IEEE Instrum. Meas. Technol. Conf.*, vol. 3, May 2005, pp. 2148–2152.
- [10] *IEEE Standard for a Precision Clock Synchronization Protocol for Networked Measurement and Control Systems*, IEEE Standard 1588-2008 (Revision of IEEE Std 1588-2002), Jul. 2008.
- [11] *Communication Networks and Systems for Power Utility Automation—Part 5: Communication Requirements for Functions and Device Models*, Standard IEC 61850-5:2013, 2013.
- [12] P. Ferrari, A. Flammini, S. Rinaldi, and G. Prytz, "Evaluation of time gateways for synchronization of substation automation systems," *IEEE Trans. Instrum. Meas.*, vol. 61, no. 10, pp. 2612–2621, Oct. 2012.
- [13] A. Mingotti, L. Peretto, and R. Tinarelli, "A novel equivalent power network impedance approach for assessing the time reference in asynchronous measurements," in *Proc. IEEE I2MTC*, May 2017, Turin, Italy, pp. 624–629.
- [14] P. Janssen, T. Sezi, and J.-C. Maun, "Distribution system state estimation using unsynchronized phasor measurements," in *Proc. IEEE ISGT Europe*, Oct. 2012, pp. 1–6.
- [15] A. L. Dalcastagne, S. N. Filho, H. H. Zurn, and R. Seara, "An iterative two-terminal fault-location method based on unsynchronized phasors," *IEEE Trans. Power Del.*, vol. 23, no. 4, pp. 2318–2329, Oct. 2008.
- [16] D. Novosel, D. G. Hart, E. Udren, and J. Garitty, "Unsynchronized two-terminal fault location estimation," *IEEE Trans. Power Del.*, vol. 11, no. 1, pp. 130–138, Jan. 1996.
- [17] C.-S. Yu, L.-R. Chang, and J.-R. Cho, "New fault impedance computations for unsynchronized two-terminal fault-location computations," *IEEE Trans. Power Del.*, vol. 26, no. 4, pp. 2879–2881, Oct. 2011.
- [18] J. Izykowski, R. Molag, E. Rosolowski, and M. M. Saha, "Accurate location of faults on power transmission lines with use of two-end unsynchronized measurements," *IEEE Trans. Power Del.*, vol. 21, no. 2, pp. 627–633, Apr. 2006.

- 527 [19] M. Fulczyk, P. Balcerek, J. Izykowski, E. Rosolowski, and M. M. Saha,  
528 "Two-end unsynchronized fault location algorithm for double-circuit  
529 series compensated lines," in *Proc. IEEE Power Energy Soc. Gen.  
530 Meeting*, Jul. 2008, pp. 1–9.
- 531 [20] B. Mahamedi and J. G. Zhu, "Unsynchronized fault location based on  
532 the negative-sequence voltage magnitude for double-circuit transmis-  
533 sion lines," *IEEE Trans. Power Del.*, vol. 29, no. 4, pp. 1901–1908,  
534 Aug. 2014.
- 535 [21] L. Yuansheng, W. Gang, and L. Haifeng, "Time-domain fault-location  
536 method on HVDC transmission lines under unsynchronized two-end  
537 measurement and uncertain line parameters," *IEEE Trans. Power Del.*,  
538 vol. 30, no. 3, pp. 1031–1038, Jun. 2015.
- 539 [22] *Voltage Characteristics of Electricity Supplied by Public Distribution  
540 Systems*, Standard IEC EN 50160:1999, 2003.
- 541 [23] C. Muscas, L. Peretto, S. Sulis, and R. Tinarelli, "Investigation on  
542 Multipoint Measurement Techniques for PQ Monitoring," *IEEE Trans.  
543 Instrum. Meas.*, vol. 55, no. 5, pp. 1684–1690, Oct. 2006.
- 544 [24] C. Muscas, "Power quality monitoring in modern electric distribution  
545 systems," *IEEE Instrum. Meas. Mag.*, vol. 13, no. 5, pp. 19–27,  
546 Oct. 2010.
- 547 [25] L. Peretto, R. Sasdelli, E. Scala, and R. Tinarelli, "Performance charac-  
548 terization of a measurement system for locating transient voltage sources  
549 in power distribution networks," *IEEE Trans. Instrum. Meas.*, vol. 58,  
550 no. 2, pp. 450–456, Feb. 2009.
- 551 [26] L. Peretto, R. Sasdelli, E. Scala, and R. Tinarelli, "Metrological charac-  
552 terization of a distributed measurement system to locate faults in power  
553 networks," in *Proc. IEEE Instrum. Meas. Technol. Conf.*, May 2008,  
554 pp. 95–100.
- 555 [27] M. Paolone, L. Peretto, R. Sasdelli, R. Tinarelli, M. Bernardi, and  
556 C. A. Nucci, "On the use of data from distributed measurement systems  
557 for correlating voltage transients to lightning," *IEEE Trans. Instrum.  
558 Meas.*, vol. 53, no. 4, pp. 1202–1208, Aug. 2004.
- 559 [28] L. Cristaldi, A. Ferrero, C. Muscas, S. Salicone, and R. Tinarelli, "The  
560 impact of Internet transmission on the uncertainty in the electric power  
561 quality estimation by means of a distributed measurement system," *IEEE  
562 Trans. Instrum. Meas.*, vol. 52, no. 4, pp. 1073–1078, Aug. 2003.
- 563 [29] A. Carullo, "Metrological management of large-scale measuring sys-  
564 tems," *IEEE Trans. Instrum. Meas.*, vol. 55, no. 2, pp. 471–476,  
565 Apr. 2006.
- 566 [30] *Instrument Transformers—Part 1: General Requirements*,  
567 Standard IEC 61869-1:2016, International Standardization Organization,  
568 Geneva, Switzerland, 2016.
- 569 [31] *Instrument Transformers—Part 6: Additional General Requirements  
570 for Low-Power Instrument Transformers*, Standard IEC 61869-6:2016,  
571 International Standardization Organization, Geneva, Switzerland, 2016.
- 572 [32] *Uncertainty of Measurement—Part 3: Guide to the Expres-  
573 sion of Uncertainty in Measurement (GUM:1995)*, Stan-  
574 dard ISO/IEC Guide 98-3:2008, International Standardization  
575 Organization, Geneva, Switzerland, 2008.
- 576 [33] *Evaluation of Measurement Data—Supplement 1 to the Guide to  
577 the Expression of Uncertainty in Measurement—Propagation of Dis-  
578 tributions Using a Monte Carlo Method*, Standard ISO/IEC Guide  
579 98-3/Suppl.1:2008, International Standardization Organization, Geneva,  
580 Switzerland, 2008.
- 581 [34] *Instrument Transformers—Part 2: Additional Requirements for Current  
582 Transformers*, Standard IEC 61869-2:2012, International Standardization  
583 Organization, Geneva, Switzerland, 2011.
- 584 [35] *Instrument Transformers—Part 3: Additional Requirements for Inductive  
585 Voltage Transformers*, Standard IEC 61869-3:2011, International Stan-  
586 dardization Organization, Geneva, Switzerland, 2011.
- 587 [36] *Fault Detection and Power Meter—Specifications and Test Methods*,  
588 (in Italian), document e-distribuzione DV7070, Nov. 2016.



**Alessandro Mingotti** (S'17) received the M.S. degree in electrical engineering from the University of Bologna, Bologna, Italy, in 2016, where he is currently pursuing the Ph.D. degree in biomedical, electrical, and systems engineering.

His current research interests include measurements for smart grids and electrical safety.



**Lorenzo Peretto** (M'98–SM'03) is currently a Professor of electrical and electronic measurements with the University of Bologna, Bologna, Italy. He is a consultant of industries operating in the field of instrumentation and sensors for electrical measurements. He has authored or co-authored over 200 papers and holds 24 patents and co-authored three books. His current research interests include the design and calibration of voltage and current instrument transformers for medium- and high-voltage power networks, the design and realization of calibration systems of voltage and current instrument transformers, and measurements of electrical quantities in power networks.

He is a member of the IEEE Instrumentation and Measurement Society. He is the Chairman of the annual IEEE Applied Measurements for Power System Conference, a member of the IEC TC38 "Instrument Transformers" and a Chairman of the TC38/WG45 "Standard Mathematical Models for Instrument Transformers" and TC38/WG53 "Uncertainty evaluation in the calibration of Instrument Transformers".



**Roberto Tinarelli** (S'02–M'05–SM'14) received the M.S. degree in electrical engineering from the University of Bologna, Bologna, Italy, in 2000, and the Ph.D. degree in electrical engineering from the Polytechnic of Milan, Italy, in 2004.

He has authored or co-authored over 120 scientific papers, one book. He is a Co-Inventor of some WO patents in the field of sensors and instrument transformers. He is currently an Associate Professor of electrical measurements with the Department "Guglielmo Marconi," University of Bologna. His

current research interests include design and metrological characterization of instruments for measurement under nonsinusoidal conditions, design and development of new instrumentation for flicker measurement, design and characterization of new electromagnetic-fields sensors and instrumentation, and reliability study of electronic devices.